CHEMISTRY JOURNAL OF MOLDOVA. General, Industrial and Ecological Chemistry. 2025, 20(2), 84-93
ISSN (p) 1857-1727 ISSN (e) 2345-1688
http://cjm.ichem.md
https://doi.org/10.19261/cjm.2025.1342

EMPLOYMENT OF *IN SILICO* IN PREDICTION OF FURAN DERIVATIVES AS EFFICIENT CORROSION INHIBITORS FOR MILD STEEL IN ACIDIC MEDIA

Maimoonah Khalid Qasim [a] and Rabah Ali Khalil [b*]

[a] *Department of New & Renewable Energy, College of Science, University of Mosul, Mosul, 41002, Iraq*
[b] *Department of Chemistry, College of Science, University of Mosul, Mosul, 41002, Iraq*
[*] *e-mail: rakhalil64@yahoo.com*

Abstract. This study highlights the role of computational approaches in advancing the design of corrosion inhibitors by virtually screening novel candidate molecules. In silico treatment based on quantitative structure-activity relationship (QSAR) analysis was performed on already published experimental results of corrosion inhibition efficiency (IE%) of mild steel in acidic media for eighteen furan derivatives. The theoretical treatments are based on density functional theory (DFT) at B3LYP level. It was found that the global minimum of the furan derivatives can be reached at a medium basis set of 6–21G. A sophisticated model consisting of four descriptors excluding the sulphur correction term with physical meaning and good statistical criteria of squared correlation coefficient (r^2) and standard error (SE) equal to 0.914 and 5.029, respectively, is presented. The suggested model can be considered as a powerful tool for understanding the role of chemical composition in preventing corrosion which helps researchers in the development process. The *in silico* treatment was utilized for suggesting twelve furan derivatives with an extremely high IE% which might be used as excellent materials for corrosion inhibition when synthesized and applied experimentally.

Keywords: furan derivative, *in silico*, corrosion inhibitor, mild steel, density functional theory.

Received: 25 July 2025/ Revised final: 07 November 2025/ Accepted: 10 November 2025

Introduction

Iron corrosion is widely recognized as a major challenge in industrial operations, leading to significant economic losses and a decline in both production efficiency and product quality. Beyond its financial impact, corrosion poses serious risks to human health and the environment, which is followed by raising safety concerns. Among the various forms of corrosion, the attack of mild steel in acidic environments is particularly important, as this material exhibits low resistance to mineral acids. In other words, chemical acids including both protic and aprotic such as hydrochloric acid (HCl) and sulphuric acid (H_2SO_4) are considered good solvent for all types of steel [1]. On the other side, corrosion inhibitors have emerged as an effective solution to overcome steel corrosion depending on the specificity of the field in which the metal is used. These inhibitors are chemical compounds that work as a protective barrier between the surface of steel and the corrosive environment which depends on their chemical composition, interaction with the metal surface, and environmental factors such as temperature and pH. Chemical inhibitors can be inorganic or organic matter as the organic is considered as modern in contrast to the historical uses of inorganic materials [2]. In general, organic inhibitors commonly contain heteroatoms such as nitrogen, sulphur, or oxygen such as furan derivatives [1–5]. The latter derivatives are considered the most common substances that are used as corrosion inhibitors for steel material. Actually, the rapid and ongoing advancements in technology have expanded the use of iron across a wide range of demanding conditions. This growing exposure has renewed scientific interest in designing and developing innovative anti-corrosion compounds to ensure long-term durability and performance. On this basis, there are several published articles concerning the inhibition of corrosion by furan derivatives [1,6–9]. Experimental investigations in this field are inherently complex, costly, and time-consuming, often relying on a trial-and-error approach. Consequently, the application of quantitative structure activity relationship (QSAR) modeling offers a promising and efficient alternative for addressing these challenges [6–12]. However, as QSAR relies primarily on statistical analyses, its outcomes must be interpreted with caution to avoid misleading conclusions. In other words, statistics is

not an exact method as that of mathematics which could give results with no regard to the correctness of the input data and to the factors that affect the subject concerned [13]. At such a point, one should bear in mind that the presented objective of statistical treatments is not captured by obtaining excellent correlation coefficient (*r*) and standard error (SE) as those can be improved by increasing the number of descriptors. Therefore, models with fewer numbers of descriptors are closer to reality, noting that, the increase in the number of observations also has bad effect towards *r* and SE which then make the model nearer to actuality. For instance, Al-Fakih, A.M. *et al.* [7] experimentally investigated the corrosion inhibition efficiency (IE%) of seventeen furan derivatives on mild steel in acidic media. The resulting data were subjected to high-dimensional QSAR analysis, which was employed primarily to identify the most relevant molecular descriptors rather than to construct a predictive model. Subsequently, Khaled, K.F. *et al.* [12] reanalysed the same experimental dataset using the semi-empirical PM3 method and developed a QSAR model based on genetic function approximation, molecular dynamics simulations, and neural network techniques. In a follow-up study, Al-Fakih A.M. *et al.* [8] extended their earlier work by developing a predictive QSAR model for the IE% of eighteen furan derivatives in acidic solution. This model was constructed using a two-stage sparse multiple linear regression approach with twelve selected descriptors. Notably, the IE% values in this study were measured with greater precision compared to their earlier work [7], as the inhibitor concentration was reduced to 0.002 M (from 0.005 M) and the polarization curve scan rate was decreased to 1 mV/s (from 10 mV/s). More recently, Hadisaputra, S. *et al.* [6] proposed a multiple linear regression (MLR) model incorporating six descriptors to predict the IE% of thirteen furan derivatives for mild steel corrosion inhibition.

The objective of this study is to propose a novel approach in the field of corrosion inhibition aimed at reducing reliance on the traditional trial and error methodology. This is achieved by developing a robust multiple linear regression (MLR) model capable of accurately predicting new, more efficient corrosion-inhibiting compounds. Importantly, the proposed MLR model is designed to retain clear physical interpretability, thereby providing valuable insights into the key factors influencing the corrosion behaviour of mild steel. To accomplish this goal, molecular descriptors of candidate compounds are first computed using the most advanced theoretical method of density functional theory (DFT) method. These descriptors are then subjected to rigorous statistical analysis to construct a reliable and predictive model. In this work, previously published data on the inhibition efficiencies (IE%) of eighteen furan derivatives for mild steel in acidic solution were adopted for further theoretical analysis [8].

Experimental

The experimental values of IE% of mild steel in acidic medium (1.0 M hydrochloric acid, HCl) for eighteen furan derivatives were taken from reference [8] as listed in Table 1 together with their names and chemical structures.

Computational methodology

The plotted two-dimensional structures of furan derivatives using ChemDraw professional version 16.0.0.82 were transferred to Chem3D Ultra version 16.0.0.82 software for theoretical processes. The package is linked with Gaussian 09w software (http://gaussian.com/g09citation/) for quantum calculations of semiempirical, ab initio (Hartree-Fock, HF) and DFT methods. The DFT was demonstrated at B3LYP level with different basis sets. The minimization of energy is considered as the most essential process in the computational aspect in order to reach global minimum in the shortest possible time particularly in using a conventional personal computer (PC). Noting that, as the less value of energy obtained from the minimization, the stereo structure of the molecule is closer to the reality [14]. Hence, the minimization process begins gradually from simplest method to the most accurate method to ensure reaching the global minimum of the compound. In other words, the minimization process starts from the molecular dynamics of MM2 (Molecular Mechanics 2) followed by the minimization of MM2, MMFF94 (Merck Molecular Force Field 94), AM1 (Austin Model 1), PM3 (Parametric Method 3), then HF and DFT methods at different basis sets (STO-3G, 3–21G, 6–21G, 4–31G, 6–31G and 6–311G). The results indicate that global minimum could be reached at 6–21G of both HF and DFT methods as shown clearly at Table 2 and Figure 1. Such a phenomenon is quite helpful in reducing the time consumed throughout the calculation process, which does not need higher basis sets. The minimization process followed by computing the properties (theoretical descriptors) for building up the QSAR model using Minitab software release 19.2020.1 (64-bit) [15,16].

Table 1

Names, chemical structures, and the experimental values of inhibition efficiency (IE%) of eighteen of furan derivates as taken from reference [8].

No	*Name*	*Chemical Structure*	*IE%*	*No*	*Name*	*Chemical Structure*	*IE%*
1	(2-2-Nitrovinyl) furan	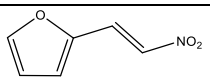	34.76	10	5-Bromo-2-furoic acid	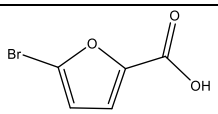	72.01
2	2-Ethyl furan	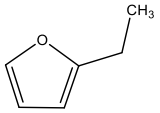	59.53	11	5-Methyl furfurylamine	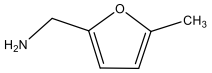	71.56
3	2-Furan methan ethiol	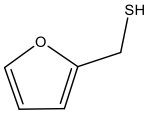	88.05	12	Ethyl 5-(Chloromethyl)-2-furoate	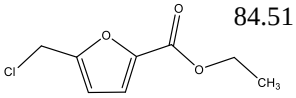	84.51
4	2-Furoic acid	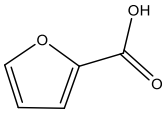	57.33	13	Methyl 5-nitro-2- furoate	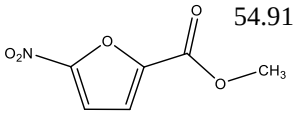	54.91
5	2-Furonitrile	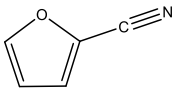	72.68	14	*trans*-3-Furanacrylic acid	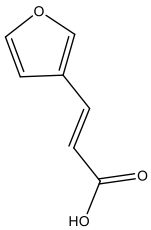	61.41
6	2-Furoyl chloride	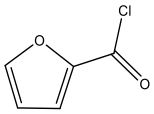	50.95	15	Furfuryl alcohol	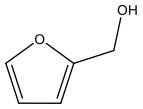	52.55
7	5-(2- Furyl)-1,3-cyclohexanedione	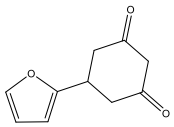	73.53	16	Furfuryl amine	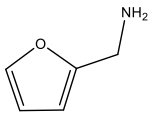	40.11
8	5-Methyl furfural	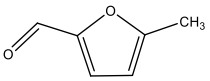	56.73	17	Methyl 2-furoate	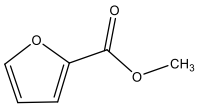	58.65
9	Dimethylaminom ethyle) furfuryl alcohole hydrochloride	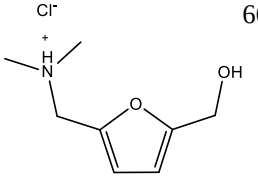	66.83	18	Methyl 2-methyl-3-furoate	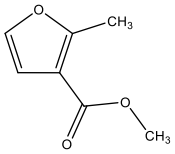	55.97

Table 2

Values of global minimum energy in Hartree unit (Eh) behind each minimization procedure at each basis set of ab initio (HF) and DFT methods.

No	*Name of compound*	*Basis set*	*HF (E_h)*	*DFT (E_h)*
1	2-2-Nitrovinyl furan	STO-3G	–502.409	–505.230
		3–21G	–506.104	–509.078
		6–21G	–508.283	–511.284
		4–31G	–508.213	–511.231
		6–31G	–508.744	–511.765
		6-311G	–508.870	–511.902
2	2-Ethyl furan	STO–3G	–302.920	–304.800
		3–21G	–304.997	–306.965
		6–21G	–306.334	–308.319
		4–31G	–306.252	–308.249
		6–31G	–306.572	–308.570
		6–311G	–306.636	–308.643

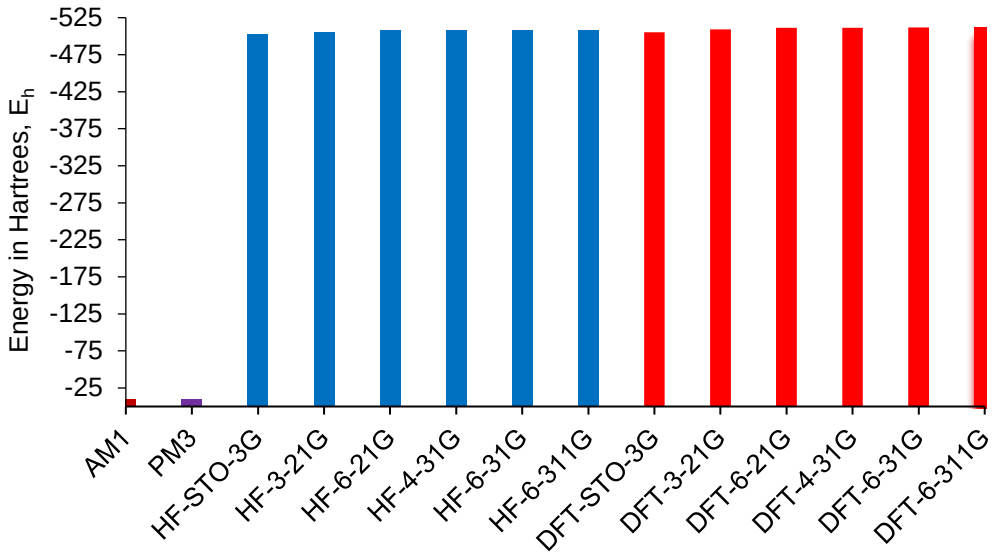

Figure 1. The effect of computational methods on different basis sets on the value of global minimum of 2-2-nitrovinyl furan (compound no. 1).

Results and discussion

When one reaches the global minimum for each compound according to the above procedure, the properties of these substances were calculated in order to be employed for building up the suggested model. Table 3 lists the values of some theoretically calculated descriptors which can be considered as examples of the several computed properties that belong to electronic and field aspects. It should be noted that the descriptors of the first effect (electronic) are mainly responsible for the chemical reactions rather than the interactions between molecules as the field effect. For instance, the first effect includes the properties of the valance electrons such as HOMO, LUMO and band gap, while the topological and charge distribution properties belong to the field effect [14-16]. Indeed, attaining an idea about the background of descriptors is considered essential due to two main reasons: dealing with the statistical aspect and obtaining a mathematical model with physical meaning that helps in understanding the factors affecting the inhibition of corrosion. Therefore, the calculated properties should first be screened using a correlation matrix to eliminate potential linear dependencies between any two descriptors, as demonstrated in Table 4. For example, the data of Table 4 show there is a relationship between ovality (Ov) and Connolly accessible area (CA) as the correlation coefficient is equal to 0.908. The statistical treatments of the theoretically calculated properties of the fifteen compounds as training set (Table 3) suggest the following model (Eq.(1)) with r^2 and SE equal to 0.914 and 5.029, respectively.

$$IE\% = -11.8 + 0.2751\,CA - 121.6\,ACO - 4.222\,NHA - 4.701\,RMSF + 21.02\,S \quad (1)$$

where, *CA* is the Connolly Accessible Area;
ACO is the average charge of oxygen;
NHA is the number of hydrogen acceptors;
RMSF is the root mean square force;
S is the sulphur atom correction term.

Noting that, this model contains only four descriptors as the last one (S) just take the value of 1 due to presence of sulphur atom at compound number 3 and zero for the rest of substituents as detailed clearly in Table 5.

Interestingly, the proposed Eq.(1) has a physical meaning through its four descriptors, as all of them are related to molecular interactions or field effect that are responsible for corrosion inhibition which therefore can be considered as unique in comparison with other related studies [6–12]. For example, the CA parameter belongs to topological properties as resulted from the area of contact surface with the solvent as sensible to the interactions with the surrounding molecules. The average charge of oxygen (ACO) and the number of hydrogen acceptors (NHA) also play a considerable role in molecular interactions through forming dipole-dipole and dipole-induced dipole forces. RMSF is considered as the basic functional form of molecular potential energy per area including both intra- and inter-molecular interactions terms. In contrast, the model reported in related work was developed primarily on a statistical basis, aiming to maximize parameters such as the correlation coefficient and minimize the standard error [12].

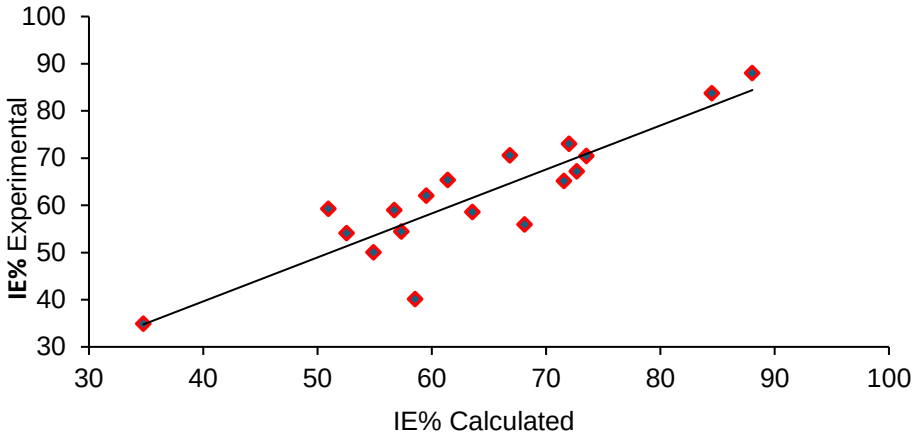

Figure 2. Experimental IE% against the calculated of the 18 furan derivatives of both training and test sets with r^2, q^2 and SE are equal to 0.7812, 0.762 and 6.412, respectively.

Table 3

Example of some from the calculated descriptors for furan derivates including Chemical Hardness (ChH), electrophilicity (Ele), Ovality (Ov), dipole moment (Dip), partition coefficient (logP), Balaban Index (BI), Wiener Index (WI), polarizability (Pol), Zero-Point Energy (Kcal/Mol) (ZPE) and logarithm of the solubility (LogS).

No	*ChH eV*	*Ele eV*	*Ov*	*Dip Debye*	*LogP*	*BI*	*WI*	*Pol A^3*	*ZEP Kcal.mol^{-1}*	*LogS Mol.l^{-1}*
Training set										
1	3.50	11.7	1.308	8.077	0.862	13184	133	151.27	70.385	–1.359
2	6.51	3.25	1.239	1.285	1.159	2089	43	73.959	84.760	–0.993
3	5.24	2.68	1.248	2.455	1.069	2089	43	92.998	65.213	–0.969
4	4.37	8.04	1.241	2.770	0.332	3936	62	78.227	56.909	–0.445
5	5.36	24.5	1.223	5.479	0.436	2089	43	84.748	46.213	–0.606
6	3.87	8.76	1.245	6.165	0.947	3936	62	91.058	47.115	–1.182
7	4.86	5.12	1.311	5.383	0.451	28775	239	125.24	122.35	–0.661
8	3.56	10.8	1.278	5.645	0.643	3991	63	89.945	72.005	–0.768
9	6.05	3.18	1.352	10.49	0.915	19979	167	120.46	147.65	–1.099
10	3.69	6.73	1.278	2.045	1.124	6981	87	107.29	50.443	–1.276
11	5.98	2.82	1.297	2.687	0.036	3991	63	78.745	96.485	–0.371
12	4.28	7.54	1.407	2.822	1.538	30155	212	131.13	107.48	–1.735
13	3.41	11.6	1.347	4.674	0.709	29052	204	120.99	76.247	–1.325
14	4.06	9.88	1.310	2.099	0.483	13184	133	128.02	79.748	–0.778
15	6.37	3.69	1.235	2.928	0.280	2089	43	63.269	69.061	0.079
Test set										
16	5.78	3.16	1.241	2.552	0.184	2089	43	66.052	77.787	–0.138
17	4.36	7.99	1.292	1.959	0.644	7142	89	92.425	75.656	–0.837
18	5.05	6.08	1.305	1.908	0.748	11488	116	93.236	94.434	–1.014

Table 4

An example of the correlation matrix between some theoretically calculated properties with experimental IE%. Noting that CA is the Connolly Accessible Area (A^2), RMSF is the root mean square force (kcal mol^{-1} Å^{-1}), ACO is the average charge of oxygen, and NHA is the number of hydrogen acceptors.

	IE%	*ChH*	*Ele*	*CA*	*Ov*	*Dip*	*RMSF*	*LogP*	*BI*	*ACO*
ChH	0.151									
Ele	–0.061	–0.426								
CA	0.337	–0.067	–0.272							
Ov	0.244	–0.315	–0.093	0.908						
Dip	–0.189	–0.139	0.253	0.387	0.250					
RMSF	–0.510	–0.657	0.268	–0.021	0.205	0.231				
LogP	0.336	–0.266	–0.054	0.397	0.402	0.066	-0.012			
BI	0.218	–0.326	0.012	0.860	0.874	0.307	0.237	0.321		
ACO	–0.389	–0.557	0.404	–0.082	0.028	0.421	0.457	0.178	0.210	
NHA	0.241	0.507	–0.548	0.756	0.538	0.269	–0.448	0.060	0.445	–0.362

Nevertheless, the resulting model was highly complex, comprising seven terms in addition to a constant. Notably, five of these terms involved ramp functions with extra coefficients, suggesting that the model was dominated by statistical fitting rather than by a physically meaningful representation. The lowest unoccupied molecular orbital (LUMO) was identified as the principal descriptor and was incorporated not only in its linear form but also as squared and cubic terms. However, the simple regression correlation coefficient (*r*) between LUMO and IE%, obtained from the correlation matrix, was only 0.02685 [12], indicating a very weak direct correlation. This observation is reasonable, as LUMO reflects an electronic parameter rather than a field effect, and no direct chemical interaction with the inhibitors is expected under these conditions.

As highlighted in the introduction, a model's predictive reliability improves as the number of included descriptors decreases. In other words, reducing the number of descriptors minimizes the likelihood of chance correlations and enhances the robustness of the prediction, in agreement with the rule proposed by Topliss and Costello [17]. The values of these descriptors together with the estimated values of IE% and the residuals between theoretical and experimental values (ΔIE%) for both training and test sets are listed in Table 5. Compound number 16 of the test set shows a relatively high residual value of 18.44 which may be related to its value of IE% as the lowest which is not suitable for use in preventing corrosion. The reason for this phenomenon may be related to the presence of amine group (NH_2) that is certainly reacted with the hydrochloric acid in order to form water soluble salt (adduct) which consequently enhances the corrosion process. On the other hand, the amino group also exists in compound number 11, but it has less effect as more hydrophobic due to the presence of methyl group which reduces the hydrophilicity of the adduct [18]. Thus, the amino group should be avoided in prediction aspect. The statistical parameters of the whole molecules (both training and test sets) including r^2, SE and Cross-validation (q^2) are equal to 0.7812, 6.412 and 0.762, respectively. The value of q^2 is above 0.5 which reflects the model strength for evaluation purpose and its ability to incorporate inside the training set [19]. The determination of the value of q^2 is clearly detailed in reference [12]. Figure 2 explains the relationship between the theoretical and observed values of IE% for all substances of 18 molecules including both training and test sets. The statistical parameters obtained in this study (r^2, q^2, and SE) are remarkably significant when compared with related work. This improvement can largely be attributed to the number of descriptors used in the model, which plays a crucial role in determining these statistical metrics.

Table 5

Values of the theoretically calculated IE% according to the suggested model of equation 1 including the related descriptors with the residuals between experimental and calculated IE%.

No	*Theoretical IE%*	*Descriptors for equation (1)*					*ΔIE% (EXP-CAL)*
		RMSF kcal mol^{-1}Å^{-1}	*NHA*	*ACO (C)*	*CA A^2*	*S*	
Training set							
1	34.88	12.17	5	–0.3573	296.34	0	–0.123
2	62.06	5.298	8	–0.4838	267.88	0	–2.528
3	88.05	6.216	6	–0.4726	275.87	1	0.000
4	54.47	10.21	4	–0.5074	252.45	0	2.862
5	67.17	6.539	3	–0.4723	236.00	0	5.512
6	59.29	8.690	3	–0.4254	264.81	0	–8.336
7	70.45	6.126	10	–0.4486	358.75	0	3.085
8	59.01	7.561	6	–0.4617	274.50	0	–2.276
9	70.57	7.478	14	–0.5324	406.66	0	–3.743
10	73.03	9.562	3	–0.5165	289.44	0	–1.024
11	65.16	6.580	9	–0.5254	297.97	0	6.404
12	83.72	7.414	9	–0.5044	388.99	0	0.791
13	50.04	12.31	5	–0.4144	328.61	0	4.872
14	65.38	9.089	6	–0.5123	301.46	0	–3.972
15	54.07	9.005	6	–0.5261	252.80	0	–1.524
Test set							
16	58.55	7.082	7	–0.5031	261.89	0	18.44
17	63.57	8.009	6	–0.4842	288.99	0	5.010
18	68.14	7.281	8	–0.5097	312.58	0	12.16

Specifically, with a dataset containing seven observations, one could theoretically achieve perfect statistical indicators (r^2= 1 and SE= 0) by employing six arbitrary descriptors that bear no actual relationship to the dependent variable [13]. In this context, the present model is constructed with only four meaningful descriptors, which demonstrates superior statistical performance compared with models utilising twelve descriptors, even when those models report a q^2 value as high as 0.95 under the same number of observations [8].

One of the main tasks of this work is to use the developed model for prediction of new more efficient compounds that could be used as corrosion inhibitor of mild steel in acidic media. Such a mission has very important advantages from a health, environmental, economic and time-consuming point of view [20]. In other words, the work within the principle of trial and error needs a lot of effort including human resources that may be a subject to chemical hazards, huge sums of money and wasting time depending on the chance of finding the target. Table 6 shows twelve proposed furan derivatives that have significant corrosion inhibition potential for mild steel in acidic environments according to the suggested model. The last Table includes the names, chemical structures, the predicted values of IE% in addition to the values of their descriptors that used as terms in the suggested model. Interestingly, the suggested compounds having very high efficiency towards corrosion according to their values of IE% which lying between 86.47 to 100.06. Moreover, only one of the suggested compounds having a value of IE% under 90% in contrast to the rest of compounds in which there are six derivatives having a value of 99.0 and over. It is noteworthy that the highest experimentally reported inhibition efficiency (IE%) among the investigated furan derivatives was 88.05% for furan methanethiol [8].

Table 6

Prediction of twelve furan derivatives of highly effective corrosion inhibitors using the suggested model of Eq.(1) with their names, chemical structures, values IE% and the calculated descriptors. Noting that, the units of the listed descriptors were already mentioned above at Table 4.

No	*Name*	*Chemical Structure*	*RMSF*	*NHA*	*ACO*	*CA*	*IE%*
1	2-(Chloromethyl)-5 (7-phenylheptyl) furan	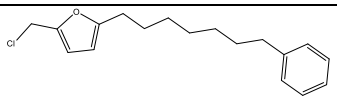	4.14	23	–0.493	609.5	99.20
2	5-(7-Chloroheptyl) furan-2-carboxylic acid	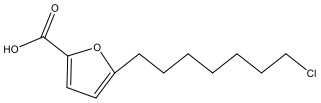	6.53	17	–0.520	499.9	86.47
3	2-Chloro-5-(7-chloroheptyl) furan	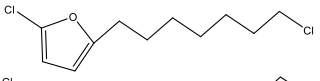	4.38	16	–0.491	479.9	91.73
4	(*E*)-2-Chloro-5-(7-chlorohept-3-en-1-yl) furan	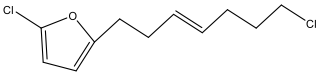	4.59	14	–0.472	476.1	95.80
5	Ethyl 5-(2-chlorovinyl) furan-2-carboxylate	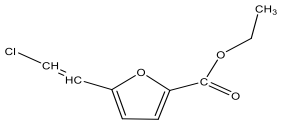	7.23	9	–0.513	405.2	90.00
6	(*E*)-2-Chloro-5-(8-chlorooct-1-en-1-yl) furan	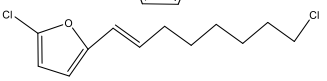	4.74	16	–0.450	507.1	98.60
7	(*E*)-2-Chloro-5-(8-chlorooct-2-en-1-yl)furan	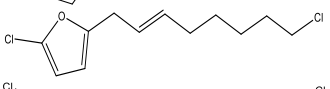	4.32	16	–0.491	511.3	100.06
8	(*E*)-2-Chloro-5-(8-chlorooct-3-en-1-yl)furan	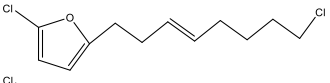	4.38	16	–0.491	506.3	99.00
9	(*E*)-2-Chloro-5-(8-chlorooct-4-en-1-yl)furan	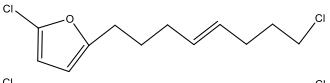	4.38	16	–0.472	510.3	97.70
10	(*E*)-2-Chloro-5-(8-chlorooct-5-en-1-yl)furan	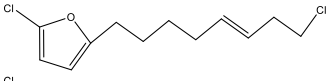	4.32	16	–0.492	507.8	99.80
11	(*E*)-2-Chloro-5-(8-chlorooct-6-en-1-yl)furan	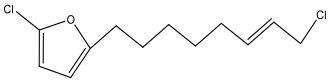	4.45	16	–0.491	510.5	99.77
12	(*E*)-2-Chloro-5-(8-chlorooct-7-en-1-yl)furan	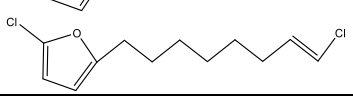	4.33	16	–0.491	508.2	99.75

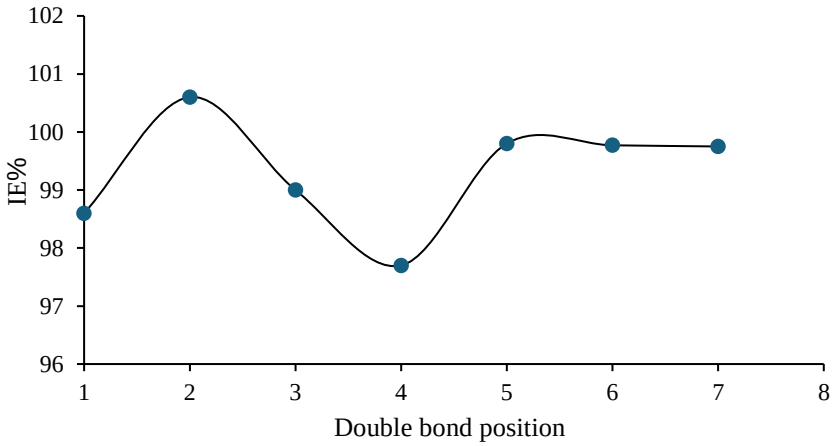

Figure 3. Effect of the position of double bond in the hydrocarbonic chain of (*E*)-2-chloro-5-(8-chlorooct-en-1-yl) furan on the corrosion inhibition (IE%) for mild steel in acidic media.

In comparison, a significantly higher IE% of 93.21% was empirically achieved by the non-furan derivative 4-hydroxybenzylideneaminomethyl -5-ethyl-1,3,4-thiadiazole at a relatively high concentration of 0.5 M [21]. The chemical structures of all suggested compounds (Table 6) possess a hydrocarbonic chain that plays a major role in acidic resistance due to its hydrophobic nature. The influence of the position of double bond with respect to the furan ring for the proposed derivatives (6–12) was investigated as clearly shown in Figure 3. A limited effect was observed at this figure as the values of IE% are lying between 97.7 to 100.06 indicating that the IE% depends on the position of π-electrons of hydrophobic chain. In general mood this may be attributed to the change in polarity and shape of the hydrocarbonic chain which depends on the position of the double bond. It should be noted that biological activity also changes with changing the position of double bond as found for omega fatty acids [22]. From an ecological standpoint, electrochemical chlorination is proposed for the synthesis of the predicted substituents, as it represents one of the most environmentally benign and sustainable methods for producing chlorinating agents [23].

Conclusions

Based on the results obtained, it can be concluded that the *in silico* approach to corrosion inhibition offers a powerful tool for advancing this field by enabling the prediction of more effective inhibitor molecules. This strategy significantly reduces reliance on traditional trial-and-error experimentation, thereby minimizing laboratory hazards, saving time, and lowering overall research costs. The application of QSAR modeling, rather than QSPR, is particularly appropriate since corrosion inhibition is more directly associated with molecular activity than with general physicochemical properties such as melting point, viscosity, or tensile strength. The proposed MLR model provides descriptors with clear physical meaning, offering valuable insights into the key factors governing corrosion inhibition mechanisms. Two main factors were identified as crucial for effective corrosion prevention of mild steel in acidic media. The first is related to molecular hydrophobicity, as the presence of a hydrophobic moiety is essential to minimize direct interaction with the acidic environment. The second involves avoiding functional groups that can react with acids to form water-soluble salts or adducts, such as amines that readily form salts with hydrochloric acid (HCl).

Acknowledgments

The authors are thankful to the University of Mosul, College of Science for supporting this research work.

References

1. Al-Mousawi, I.M.H.; Ahmed, R.S.; Kadhim, N.J.; Farhan, A.M. Study of corrosion inhibition for mild steel in hydrochloric acid solution by a new furan derivative. Journal of Physics: Conference Series, 2021, 1879, 022061, pp. 1–11. DOI: https://doi.org/10.1088/1742-6596/1879/2/022061
2. Guimarães, T.A.S.; da Cunha, J.N.; de Oliveira, G.A.; da Silva, T.U.; de Oliveira, S.M.; de Araújo, J.R.; de P. Machado, S.; D'Elia, E.; Rezende, M.J.C. Nitrogenated derivatives of furfural as green corrosion inhibitors for mild steel in HCl solution. Journal of Materials Research and Technology, 2020, 9(4), pp. 7104–7122. DOI: https://doi.org/10.1016/j.jmrt.2020.05.019

3. Khaled, K.F. Understanding corrosion inhibition of mild steel in acid medium by some furan derivatives: A comprehensive overview. Journal of the Electrochemical Society, 2010, 157(3), pp. C116–C124. DOI: https://doi.org/10.1149/1.3274915
4. Manh, T.D.; Huynh, T.L.; Thi, B.V.; Lee, S.; Yi, J.; Nguyen Dang, N. Corrosion inhibition of mild steel in hydrochloric acid environments containing *Sonneratia caseolaris* leaf extract. ACS omega, 2022, 7(10), pp. 8874–8886. DOI: https://doi.org/10.1021/acsomega.1c07237
5. Chaouiki, A.; Lgaz, H.; Chung, I.-M.; Ali, I.H.; Gaonkar, S.L.; Bhat, K.S.; Salghi, R.; Oudda, H.; Khan, M.I. Understanding corrosion inhibition of mild steel in acid medium by new benzonitriles: insights from experimental and computational studies. Journal of Molecular Liquids, 2018, 266, pp. 603–616. DOI: https://doi.org/10.1016/j.molliq.2018.06.103
6. Hadisaputra, S.; Irham, A.D.; Purwoko, A.A.; Junaidi, E.; Hakim, A. Development of QSPR models for furan derivatives as corrosion inhibitors for mild steel. International Journal of Electrochemical Science, 2023, 18(8), 100207, pp. 1–10. DOI: https://doi.org/10.1016/j.ijoes.2023.100207
7. Al-Fakih, A.M.; Aziz, M.; Abdallah, H.H.; Algamal, Z.Y.; Lee, M.H.; Maarof, H. High dimensional QSAR study of mild steel corrosion inhibition in acidic medium by furan derivatives. International Journal of Electrochemical Science, 2015, 10(4), pp. 3568–3583. DOI: https://doi.org/10.1016/S1452-3981(23)06562-8
8. Al-Fakih, A.M.; Algamal, Z.Y.; Lee, M.H.; Abdallah, H.H.; Maarof, H.; Aziz, M. Quantitative structure–activity relationship model for prediction study of corrosion inhibition efficiency using two-stage sparse multiple linear regression. Journal of Chemometrics, 2016, 30(7), pp. 361–368. DOI: https://doi.org/10.1002/cem.2800
9. Al-Fakih, A.M.; Abdallah, H.H.; Maarof, H.; Aziz, M. Experimental and quantum chemical calculations on corrosion inhibition of mild steel by two furan derivatives. Jurnal Teknologi (Sciences & Engineering), 2016, 78(6–12), pp. 121–125. DOI: https://doi.org/10.11113/jt.v78.9242
10. Idrissi, M.B.; Moumen, I.; Taghzouti, S.; Sayin, K.; Chakir, E.M.; Zarrok, H.; Oudda, H. Harnessing machine learning for QSPR modeling of corrosion inhibitors in HCl for mild steel protection. Current Analytical Chemistry, 2025, 21(4), pp. 356–373. DOI: http://doi.org/10.2174/0115734110312696240822101941
11. Ferigita, K.S.M.; Saracoglu, M.; AlFalah, M.G.K.; Yilmazer, M.I.; Kokbudak, Z.; Kaya, S.; Kandemirli, F. Corrosion inhibition of mild steel in acidic media using new oxo-pyrimidine derivatives: Experimental and theoretical insights. Journal of Molecular Structure, 2023, 1284, 135361, pp. 1–19. DOI: https://doi.org/10.1016/j.molstruc.2023.135361
12. Khaled, K.F.; Al-Nofai, N.M.; Abdel-Shafi, N.S. QSAR of corrosion inhibitors by genetic function approximation, neural network and molecular dynamics simulation methods. Journal of Materials and Environmental Science, 2016, 7(6), pp. 2121–2136. https://www.jmaterenvironsci.com/Document/vol7/vol7_N6/227-JMES-2309-Khaled.pdf
13. Shahab, Y.A.; Khalil, R.A. A new approach to NMR chemical shift additivity parameters using simultaneous linear equation method. Spectrochimica Acta Part A, 2006, 65(2), pp. 265–270. DOI: https://doi.org/10.1016/j.saa.2005.10.041
14. Khalil, R.A. A Simple Approach to Quantum Chemistry. Nova Science Publishers: New York, 2020, 139 p. https://novapublishers.com/shop/a-simple-approach-to-quantum-chemistry/
15. Khalil, R.A.; Zarari, A.H.A. *In Silico* treatment for prediction of new effective pesticides based on acetylcholinesterase inhibition. Doklady Chemistry, 2024, 518, pp. 154–165. DOI: https://doi.org/10.1134/S0012500825600038
16. Khalil, R.; Abdulrahman, S.H. A developed QSPR model for the melting points of isatin derivatives. Turkish Computational and Theoretical Chemistry, 2022, 6(1), pp. 1–8. DOI: https://doi.org/10.33435/tcandtc.894168
17. Khan, K.; Abdullayev, R.; Jillella, G.K.; Nair, V.G.; Bousily, M.; Kar, S.; Gajewicz-Skretna, A. Decoding cyanide toxicity: Integrating Quantitative Structure-Toxicity Relationships (QSTR) with species sensitivity distributions and q-RASTR modeling. Ecotoxicology and Environmental Safety, 2025, 291, 117824, pp. 1–15. DOI: https://doi.org/10.1016/j.ecoenv.2025.117824
18. Xu, Z.; Lin, S.; Li, Q.; Jiang, S.; Wang, P. Recent advances in techniques for enhancing the solubility of hydrophobic drugs. Pakistan Journal of Pharmaceutical Sciences, 2022, 35(1), pp. 95–112. https://www.pjps.pk/uploads/pdfs/35/1/Paper-14.pdf
19. Wieczorek, J.; Lei, J. Model selection properties of forward selection and sequential cross-validation for high-dimensional regression. The Canadian Journal of Statistics, 2022, 50(2), pp. 454–470. DOI: https://doi.org/10.1002/cjs.11635
20. Khalil, R.A.; Abdulrahman, S.H. Newly developed statistically intensive QSAR models for biological activity of isatin derivatives. Studia Universitatis Babes-Bolyai Chemia, 2022, 67(1), pp. 139–152. DOI: https://doi.org/10.24193/subbchem.2022.1.09

21. Habeeb, H.J.; Luaibi, H.M.; Dakhil, R.M.; Kadhum, A.A.H.; Al-Amiery, A.A.; Gaaz, T.S. Development of new corrosion inhibitor tested on mild steel supported by electrochemical study. Results in Physics, 2018, 8, pp. 1260–1267. DOI: https://doi.org/10.1016/j.rinp.2018.02.015
22. Hayashi, D.; Mouchlis, V.D.; Dennis, E.A. Omega-3 versus Omega-6 fatty acid availability is controlled by hydrophobic site geometries of phospholipase A_2s. Journal of Lipid Research, 2021, 62, 100113, pp. 1–13. DOI: https://doi.org/10.1016/j.jlr.2021.100113
23. Engbers, S.; Hage, R.; Klein, J.E.M.N. Toward environmentally benign electrophilic chlorinations: from chloroperoxidase to bioinspired isoporphyrins. Inorganic Chemistry, 2022, 61(21), pp. 8105–8111. DOI: https://doi.org/10.1021/acs.inorgchem.2c00602